Controlled Assembly of Nanoparticle-Containing Gold and Silica Microspheres and Silica/Gold Nanocomposite Spheroids with Complex Form

Alexander Kulak, Sean A. Davis, Erik Dujardin, and Stephen Mann*

School of Chemistry, University of Bristol, Bristol BS8 1TS, United Kingdom

Received July 17, 2002. Revised Manuscript Received October 4, 2002

Sonication of microliter volumes of aqueous silica, gold, or silica/gold colloids in toluene results in solidification within dissolving water droplets and the facile preparation of nanoparticle-based microspheres. At 0 and 10 °C, smooth spheres with mean diameters of 0.5 and 0.75 μm, respectively, are produced for samples prepared from gold or silica nanoparticles. In contrast, nanocomposite spheroids prepared from 2:1 silica/gold mixtures exhibit unusual surface textures due to higher-order aggregation between microspheres undergoing solidification. At 0 °C, binary collisions between similar sized droplets produce fused pairs that solidify and subsequently fragment into 0.5-μm-sized silica/gold microspheres with a pitted olive morphology consisting of a single circular indentation. Larger spheroids with multiple surface indentations and holes are produced for droplets of disparate size, for example at 10−20 °C or at 0−5 °C when the sonication time or water content are reduced to <3 min and <20 μL/100 mL, respectively. A wide range of nanoparticle-containing microspheres with complex morphology and multi-functionality for use in catalysis, separation science, and bioengineering should be accessible by development of the procedures described.

Introduction

The controlled construction of organized matter using nanoparticle building blocks − *nanotectonics*[1,2] − represents a new challenge in materials research with potential spin-offs in many macroscopic devices.[3,4] From an engineering perspective, nanotectonics is a miniaturization problem dealing with assembly, patterning, and device integration, whereas in terms of synthesis it requires new developments in "chemistry beyond the supermolecule".[5] The multiscale ordering, interlinking, and interfacing of discrete nanoparticles requires increased levels of informational content and this can be provided internally through programmed assembly[6] or externally using a wide variety of templates.[2]

Programmed assembly involves the self-coding of nanoparticle building blocks that can be coupled via interparticle connectors with specific recognition properties based on, for example, DNA duplex formation,[7] antibody−antigen specificity,[8] streptavidin−biotin coupling,[9] electrostatic matching,[10] or shape-directed hydrophobic forces.[11] In contrast, template-directed methods utilize porous solid substrates or discrete liquid droplets as patterned or shaped interfaces for the assembly of preformed nanoparticles. For example, a range of monoliths with macroporous architectures have been produced by nanoparticle infiltration of the ordered void spaces of polystyrene latex or silica colloidal crystals with aluminum phosphate,[12] CdSe,[13] TiO_2 and SiO_2,[14] or Au[15,16] dispersions. Similar methods have been employed with polymer sponge templates using Fe_3O_4 or TiO_2 nanoparticles,[17] as well as biological architectures such as bacterial multicellular threads (SiO_2, silicalite),[18] sea urchin skeletons ($CaCO_3$),[19] and starch gels and sponges (silicalite).[20] In each case,

* To whom correspondence should be addressed. Phone: +44-117-928-9935. Fax: +44-117-929-0509. E-mail: s.mann@bristol.ac.uk.

(1) Mann, S.; Davis, S. A.; Hall, S. R.; Li, M.; Rhodes, K. H.; Shenton, W.; Vaucher, S.; Zhang, B. *Dalton Trans.* **2000**, 3753.
(2) Davis, S. A.; Breulmann, M.; Rhodes, K. H.; Zhang, B.; Mann, S. *Chem. Mater.* **2001**, *13*, 3218.
(3) Collier, C. P.; Vossmeyer, T. V.; Heath, J. R. *Annu. Rev. Phys. Chem.* **1998**, *49*, 371.
(4) Shipway, A. N.; Katz, E.; Willner, I. *ChemPhysChem* **2000**, *1*, 18.
(5) To paraphrase J.-M. Lehn. Lehn, J.-M. *Supramolecular Chemistry*; VCH: Weinheim, Germany, 1995.
(6) Mann, S.; Shenton, W.; Li, M.; Connolly, S.; Fitzmaurice, D. *Adv. Mater.* **2000**, *12*, 147.
(7) (a) Mirkin, C. A.; Letsinger, R. L.; Mucic, R. C.; Storhoff, J. J. *Nature* **1996**, *382*, 607. (b) Alivasatos, P.; Johnsson, K. P.; Peng, X.; Wilson, T. E.; Loweth, C. J.; Bruchez, M.; Schultz, P. G. *Nature* **1996**, *382*, 609. (c) Shipway, A. N.; Willner, I. *Chem. Commun.* **2001**, 2035. (d) Josephson, L.; Perex, J. M.; Weissleder, R. *Angew. Chem., Int. Ed.* **2001**, *40*, 3204. (e) Dujardin, E.; Hsin, L.-B.; Wang, C. R. C.; Mann, S. *Chem. Commun.* **2001**, 1264.
(8) Shenton, W.; Davis, S. A.; Mann, S. *Adv. Mater.* **1999**, *11*, 449.
(9) (a) Connolly, S.; Fitzmaurice, D. *Adv. Mater.* **1999**, *11*, 1202. (b) Li, M.; Wong, K. K. W.; Mann, S. *Chem. Mater.* **1999**, *11*, 23.
(10) (a) Galow, T. H.; Boal, A. K.; Rotello, V. M. *Adv. Mater.* **2000**, *8*, 576. (b) Boal, A. K.; Galow, T. H.; Ilhan, F.; Rotello, V. M. *Adv. Funct. Mater.* **2001**, *11*, 461.
(11) Li, M.; Schnablegger, H.; Mann, S. *Nature* **1999**, *402*, 393.
(12) Holland, B. T.; Blanford, C. F.; Do, T.; Stein, A. *Chem. Mater.* **1999**, *11*, 795.
(13) Vlasov, Y. A.; Yao, N.; Norris, D. J. *Adv. Mater.* **1999**, *11*, 165.
(14) Subramania, G.; Manoharan, V. N.; Thorne, J. D.; Pine, D. J. *Adv. Mater.* **1999**, *11*, 1261.
(15) Velev, O. D.; Tessier, P. M.; Lenhoff, A. M.; Kaler, E. W. *Nature* **1999**, *401*, 548.
(16) Velev, O. D.; Kaler, E. W. *Adv. Mater.* **2000**, *12*, 531.
(17) Breulmann, M.; Davis, S. A.; Mann, S.; Hentze, H. P.; Antonietti, M. *Adv. Mater.* **2000**, *12*, 502.

10.1021/cm021259e CCC: $25.00
Published on Web 01/04/2003

capillary, drying, or swelling forces are used to implant, position, and fix the nanoparticles irreversibly within the template. In contrast, specific chemical interactions are used to assemble nanoparticles, such as silica,[21] silicalite,[22] CdTe(S),[23] or Au[24] around the surface of individual latex beads precoated with a layer-by-layer shell of oppositely charged polyelectrolyte macromolecules.

Dispersed droplets of water or oil can be used as liquid templates for the preparation of hollow inorganic microspheres either by spray drying[25,26] or interfacial reactions in microemulsions.[27−29] There are few reports, however, describing the interfacial assembly of preformed nanoparticles at droplet surfaces. Recently, exfoliated clay sheets have been organized around the surface of mini-emulsion droplets,[30] and remarkable spheroidal structures have been prepared by sonication of zeolite crystals with well-defined morphologies in water-in-oil emulsions.[31] In this paper, we develop and extend the latter approach to spheroidal architectures based on assembled nanoparticles with metallic (Au), ceramic (SiO_2), or composite (Au/SiO_2) properties. In contrast to previous investigations, which used zeolite crystallites, ca. 250 nm size, we use hydrophilic nanoparticles with dimensions of 3−4 nm (Au) or 12−14 nm (SiO_2), and show that combinations of these building blocks influence the interfacial properties of the assembled structures to produce solid, hollow, indented, or perforated spheroids. Unlike previous studies in which spheroidal architectures with complex form have been prepared by latex bead templating in spray dried droplets,[26] phase-separation[27] or CO_2 microbubble templating in microemulsions,[28] or time-dependent sonication in surfactant-stabilized emulsion droplets,[31] the morphologies described here are generated by higher-order collisional processes. These are determined by the interfacial properties, polydispersity, and aggregation behavior of the nanoparticle-based spheroids, and are controlled experimentally by changes in composition, temperature, water content, and sonication time. The experimental procedure is facile and should therefore be of general use in the preparation of multi-functional nanoparticle-containing microspheres with complex form. Such materials should have generic applications, for example in catalysis, separation science, and bioengineering.

Experimental Section

Nanoparticle Synthesis. Hydrophilic gold nanoparticles were prepared as described previously.[32] Briefly, an aqueous sodium borohydride solution (25 mL, 0.2 M) was added at a rate of 2.5 mL per min to 100 mL of methanol containing 5 mM $HAuCl_4$ and 1.25 mM of mercaptosuccinic acid under vigorous stirring. After reaction, the particles were repeatedly washed with 20%(v/v) water/methanol, methanol, and ethanol solutions using an ultrasonic dispersion−centrifugation process to remove inorganic or organic impurities. The final product was dried under vacuum to produce a dry black powder. TEM studies showed discrete spherical nanoparticles with a mean particle size of 3−4 nm.

Microsphere Preparation. Microspheres consisting of compacted gold nanoparticles were prepared by addition of toluene (100 mL) to a plastic bottle (250 mL capacity) containing a dispersion of succinate-capped gold nanoparticles in water (typically, 10 mg in 20 μL), followed by sonication of the mixture for 5 min using a 600 W probe sonicator (Misonix XL2020) with tip diameter of 3.5 mm at 15% power under air. Samples were prepared at temperatures of 0, 5, 10, or 15 °C (±1 °C) using an ethanol/dry ice bath. The bottle was removed from the sonicator and allowed to warm to room temperature (0.5 h). Samples were prepared for SEM and TEM studies by air-drying droplets of the suspension onto aluminum stubs and carbon-coated copper grids, respectively.

Silica microspheres were prepared as above except that 25 mg (ca. 10 mg SiO_2, 15 μL water) of a 40 wt % aqueous suspension of 12−14-nm-sized silica nanoparticles (pH 9−10.5, Snowtex 40, Nissan Chemical Industry) was used in place of the aqueous gold sol.

Microspheres comprising a 2:1 weight ratio of silica and gold nanoparticles were prepared as above but using 35 μL of an aqueous phase typically consisting of 25 mg (10 mg SiO_2, 15 μL water) of a Snowtex 40 dispersion and 5 mg of succinate-capped gold nanoparticles suspended in 20 μL of water. Most experiments were undertaken at 0 or 10 °C with a sonication time of 5 min, although times of 1, 2.5, 10, and 30 min were also investigated. The experiments were repeated with the same total solids content but different SiO_2:Au weight ratios (1:10, 1:2, 1:1, and 10:1), and at higher (95 μL) or lower (17.5 μL) water contents at a fixed SiO_2/Au ratio of 2:1.

Characterization. Samples were investigated using a JEOL JSM 5600 LV SEM and JEOL 1200EX TEM equipped with EDXA facilities (Oxford Instruments, ISIS300). Microspheres were calcined at 450 °C for 12 h in a ELF 11/6 Carbolite oven.

Results and Discussion

Microspheres Prepared from Gold or Silica Nanoparticles. Sonication of milligram quantities of succinate-capped gold nanoparticles in 100 mL of toluene containing 20 μL of water for 5 min at temperatures between 0 and 15 °C, followed by warming to room temperature, produced a transparent solution and black-brown sediment. SEM micrographs of the redispersed precipitate showed a high yield (>95%) of metallic microspheres (Figure 1a). Similar results were obtained when 25 mg (10 mg SiO_2, 15 μL of water) of a dispersion of amorphous silica nanoparticles was sonicated in toluene (Figure 1b). In both cases, the spheroids

(18) (a) Davis, S. A.; Burkett, S. L.; Mendelson, N. H.; Mann, S. *Nature* **1997**, *385*, 420. (b) Zhang, B.; Davis, S. A.; Mendelson, N. H.; Mann, S. *Chem. Commun.* **2000**, 781.
(19) Seshadri, R.; Meldrum, F. C. *Adv. Mater.* **2000**, *12*, 1149.
(20) Zhang, B.-Z.; Davis, S. A.; Mann, S. *Chem. Mater.* **2002**, *14*, 1369.
(21) Caruso, F.; Caruso, R. A.; Möhwald, H. *Science* **1998**, *282*, 1111.
(22) (a) Rhodes, K. H.; Davis, S. A.; Caruso, F.; Zhang, B.; Mann, S. *Chem. Mater.* **2000**, *12*, 2832. (b) Wang, X. D.; Yang, W. L.; Tang, Y.; Wang, Y. J.; Fu, S. K.; Gao, Z. *Chem. Commun.* **2000**, 2161.
(23) Rogach, A.; Susha, A.; Caruso, F.; Sukhorukov, G.; Kornowski, A.; Kershaw, S.; Möhwald, H.; Eychmüller, A.; Weller, H. *Adv. Mater.* **2000**, *12*, 333.
(24) Gittens, D. I.; Susha, A. S.; Schoeler, B.; Caruso, F. *Adv. Mater*, **2002**, *14*, 508.
(25) Brusinsma, P. J.; Kim, A. Y.; Liu, J.; Baskaran, S. *Chem. Mater.* **1997**, *9*, 2507.
(26) Iskandar, F.; Mikrajuddin, F. I.; Okuyama, K. *Nanoletters* **2002**, *2*, 389.
(27) Walsh, D.; Mann, S. *Nature* **1995**, *377*, 320.
(28) Walsh, D.; Lebeau, B.; Mann, S. *Adv. Mater.* **1999**, *11*, 324.
(29) (a) Schacht, S.; Huo, Q.; Voigt-Martin, I. G.; Stucky, G. D.; Schüth, F. *Science* **1996**, *273*, 768. (b) Jafeliccit, M., Jr.; Davolos, M. R.; Jose de Santos, F.; Jose de Santos, A. *J. Non-Cryst. Solids*. **1999**, *247*, 98. (c) Fowler, C. E.; Khushalani, D.; Mann, S. *J. Mater. Chem.* **2001**, *11*, 1968. (d) Fowler, C. E.; Khushalani, D.; Mann, S. *Chem. Commun.* **2001**, 2028.
(30) zu Putlitz, B.; Landfester, K.; Fischer, H.; Antonietti, M. *Adv. Mater.* **2001**, *13*, 500.
(31) Kulak A.; Lee, Y.-J.; Park, Y. S.; Kim, H. S.; Lee, G. S.; Yoon, K. B. *Adv. Mater.* **2002**, *14*, 526.
(32) Chen, S.; Kimura, K. *Langmuir* **1999**, *15*, 1075.

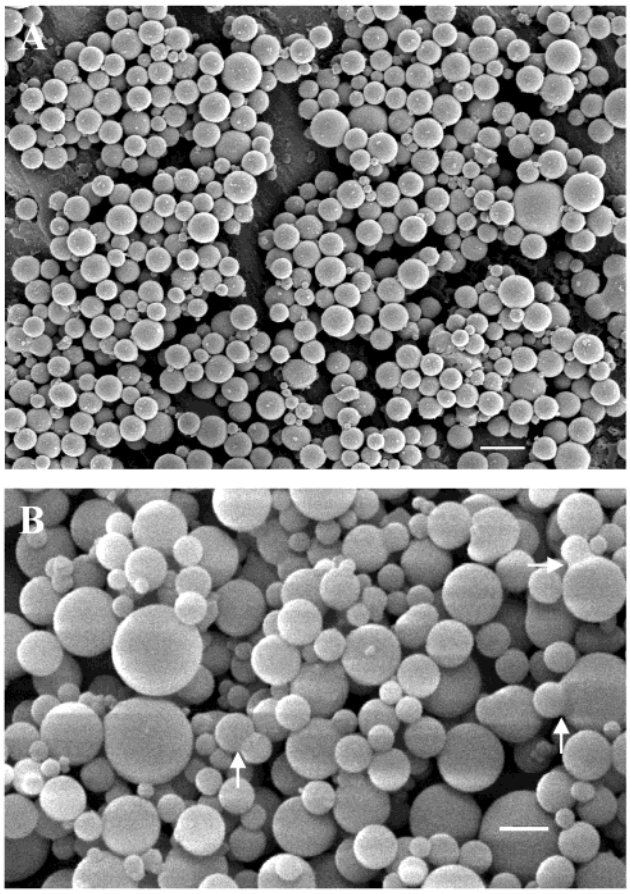

Figure 1. SEM images of microspheres assembled from (a) gold and (b) silica nanoparticles. Fused pairs of silica microspheres are shown by arrows in (b). Scale bars = 1 μm.

had smooth continuous external surfaces and solid interiors, although hollow microspheres were occasionally observed for the silica materials. A small percentage of the silica microspheres were fused into pairs (Figure 1b, arrows), whereas the gold microspheres were always discrete. At 0 °C, more than 90% of the gold or silica microspheres were sized between 0.25 and 0.75 μm (mean diameters: Au, 0.5 μm, $\sigma = 0.19$; SiO_2, 0.5 μm, $\sigma = 0.23$); in contrast, raising the temperature to 10 °C increased the mean diameters to 0.75 μm and broadened the particle size distribution significantly (Figure 2). Reducing the sonication time to less than 3 min at 0 °C also increased the size and polydispersity of the gold or silica microspheres, whereas increased sonication times had negligible effect on the size distribution. Significantly, although the gold microspheres could be isolated by filtration in toluene and readily manipulated as dry powders, they readily disassembled in polar solvents such as ethanol and water, or when heated to moderate temperatures (450 °C). The silica microspheres, in contrast, were stable in polar solvents and remained intact after calcination at 450 °C for 12 h.

The above results are consistent with a general mechanism involving the consolidation of hydrophilic nanoparticles within micrometer-sized aqueous droplets present in the sonicated toluene/water mixture (Figure 3).[31] The packing density of the nanoparticles at the water/oil interface and within the water drops is increased progressively as the droplet volume decreases due to dissolution of the water phase in toluene (water

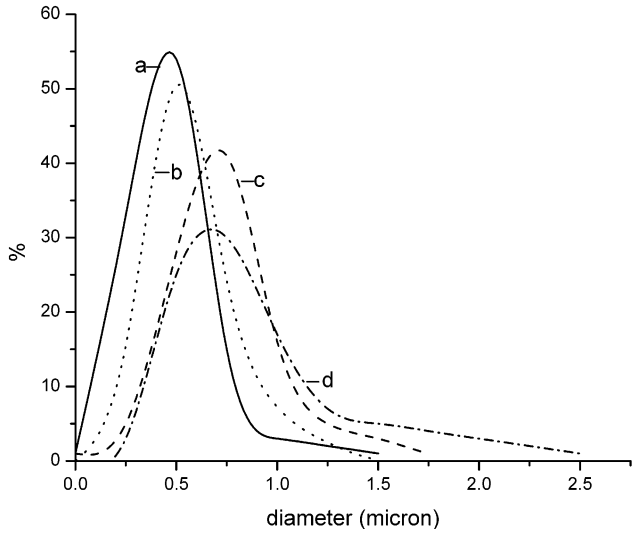

Figure 2. Particle size distributions for (a) gold microspheres prepared at 0 °C, (b) silica microspheres at 0 °C, (c) gold microspheres at 10 °C, and (d) silica microspheres at 10 °C.

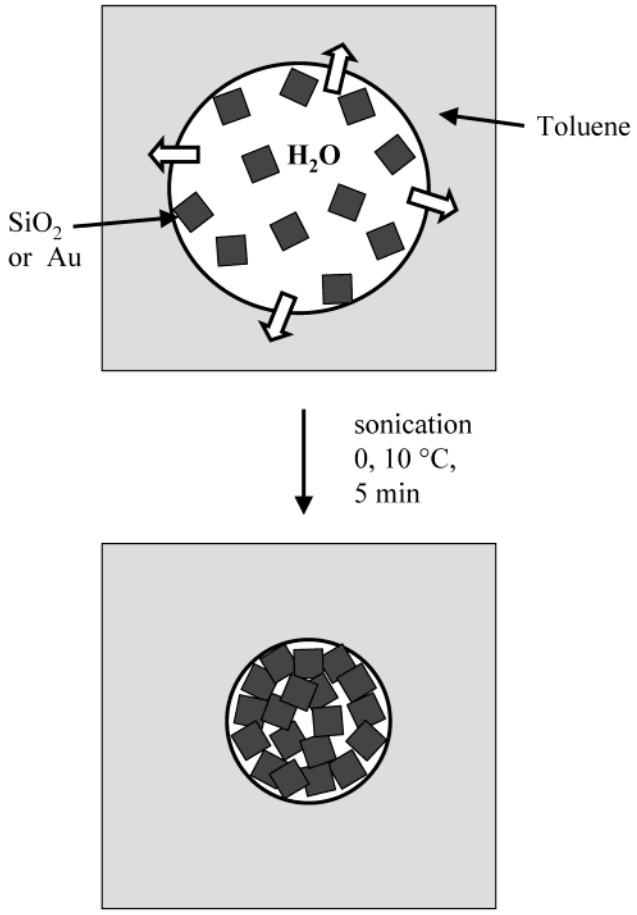

Figure 3. Scheme showing nanoparticle solidification in water droplets dispersed in toluene. Open arrows represent water flux due to dissolution.

solubility = 0.047% at 20 °C). Moreover, the rate of solidification is dependent on the rate and extent of droplet dissolution, which are sufficiently low at 0 °C that monodispersed droplets of the nanoparticle sols are produced, provided that the sonication time is long enough (>3.5 min) to establish a homogeneous emulsion. At higher temperatures (>10 °C), the increased rate of dissolution and water solubility result in faster

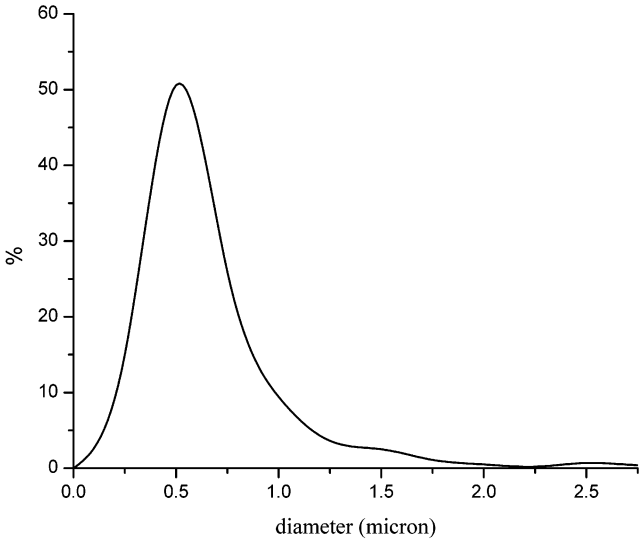

Figure 4. Particle size distribution for silica/gold microspheres prepared at 0 °C.

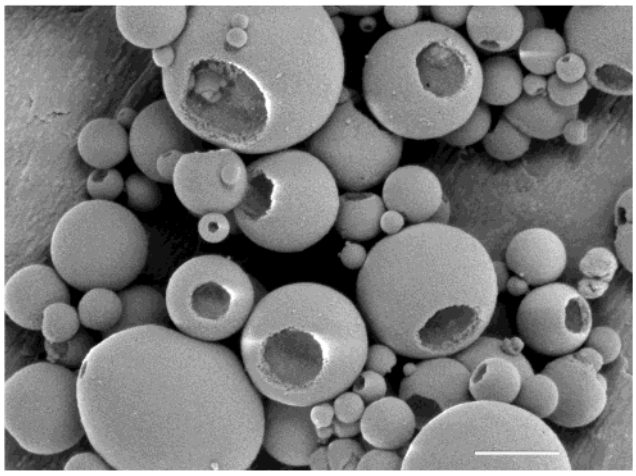

Figure 5. SEM image showing silica/gold microspheres with pitted olive morphology prepared at 0 °C with 35 μL of water. Scale bar = 1 μm.

solidification such that the nanoparticle-based microspheres form prior to homogenization, that is, within droplets that are generally larger and less uniform in size. The assembly process is reversible for the gold microspheres because the succinate-capped nanoparticles are held together principally by capillary forces that are readily overcome by solvation and heating. In contrast, the silica spheres consist of a silica gel of cross-linked nanoparticles (see below, Figure 6b) that stabilizes the microstructure. Condensation of Si−OH groups on the nanoparticle surfaces could arise by increases in the ionic strength as the water droplets dissolve in toluene, or by sonication-induced interparticle siloxane bridges,[31] or both.

Silica/Gold Nanocomposite Microspheres. Microspheres were prepared by sonicating water/toluene dispersions containing typically 35 μL/100 mL of silica and gold nanoparticles at a SiO_2/Au weight ratio of 2:1. Sonication for 5 min at 0−5 °C produced intact polydisperse microspheres (mean diameter, 0.5 μm, $\sigma = 0.23$) (Figure 4) that were stable in polar solvents or when heated to 450 °C for 12 h. Surprisingly, SEM studies showed remarkable changes in the surface texture and porosity for the SiO_2/Au microspheres compared with

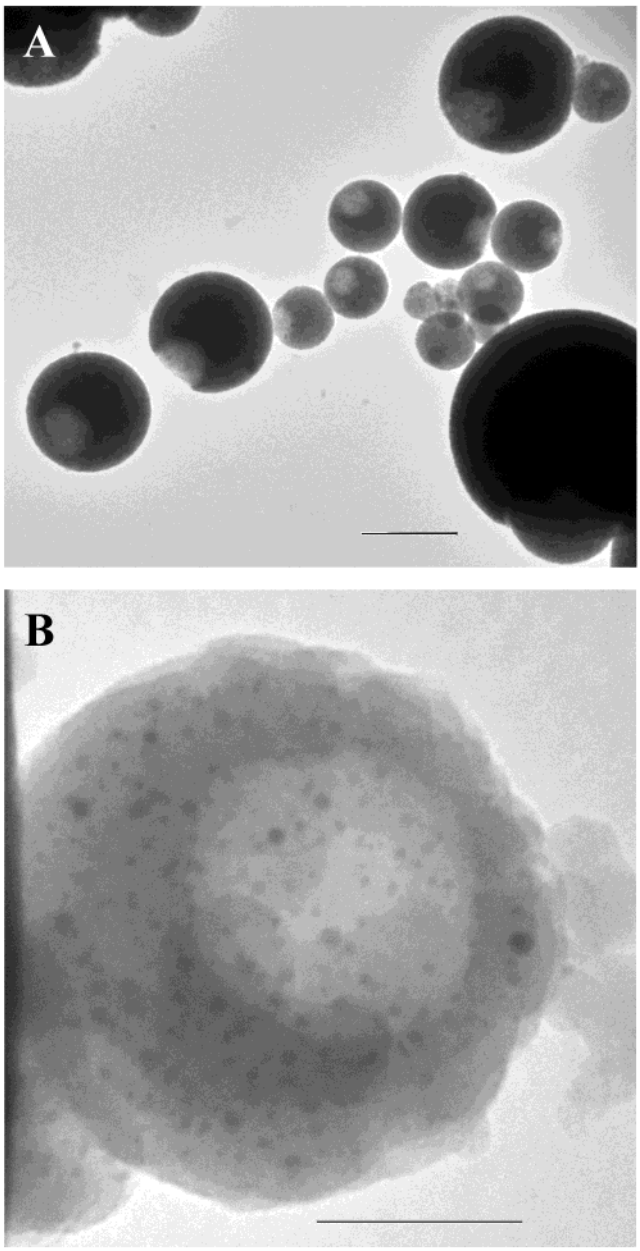

Figure 6. TEM micrographs of silica/gold nanocomposite microspheres prepared at 0 °C with 35 μL of water. (a) Low magnification view of pitted olive spheroids, scale bar = 500 nm; (b) high magnification image of single microsphere showing discrete gold nanoparticles embedded in a cross-linked silica gel matrix, scale bar = 50 nm.

those prepared from silica or gold alone. The composite microspheres exhibited an unusual "pitted olive" morphology consisting of a single circular indentation of variable diameter and depth (Figure 5). In most cases, the internal surface of the indentation and outer surface of the microsphere were smooth, but the crater edges were irregular. TEM images and EDX analysis of spheroids indicated that the microspheres consisted of discrete Au nanoparticles distributed homogeneously within a continuous silica gel matrix (Figure 6). Occasionally, pairs of partially fused particles were observed in the SEM images suggesting that the pitted olive morphology originated from binary collisions between the incipient water-containing microspheres followed by solidification and fragmentation at the point

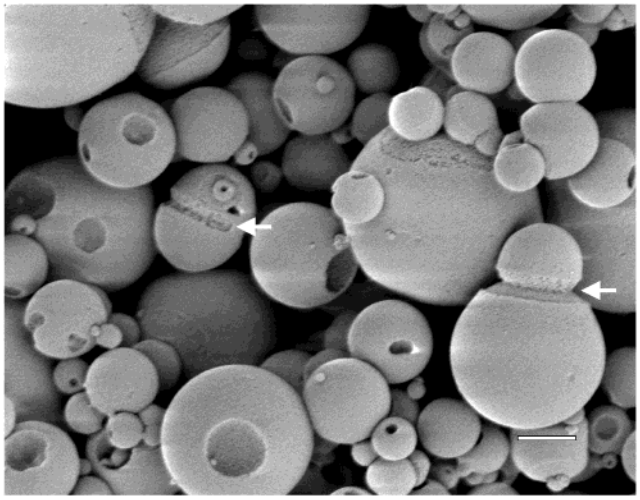

Figure 7. Silica/gold microspheres prepared at 0 °C with 95 μL of water showing fused pairs (arrows) with significant disruption of the surface structure at the contact points. Scale bar = 1 μm.

of contact to reveal the circular indentation or hole. Increasing the number of droplets in the mixture by changing the water content from 35 to 95 μL produced a significant increase in the number of fused pairs of microspheres observed by SEM (Figure 7), whereas lower water droplet concentrations gave smooth spheres without the pitted olive morphology. The observations are therefore consistent with a collision-based mechanism. Interestingly, unlike the fused pairs of pure silica microspheres shown in Figure 1b, the silica/gold structures showed extensive surface disruption at the contact points between conjoined particles (Figure 7, arrows), suggesting significant changes in the surface texture and mechanical properties in the composite materials.

Remarkable changes in microsphere morphology were observed when mixtures were sonicated for 5 min at 0−5 °C with the water content reduced to 17.5 μL. The product consisted of highly polydisperse silica/gold spheroids that were up to 10 μm or so in diameter. Although the pitted olive morphology was retained for the smaller microspheres, the larger spheroids consisted of multiple surface indentations with circular profiles (Figure 8). The indentations were discrete, nonuniform in size, randomly distributed, and sometimes perforated to reveal a hollow interior. Occasionally, small spheres were observed fused to the outer surface of the large microspheres (Figure 8, arrows), indicating that the surface pockmarks and perforations originated from multiple collisions between hollow/solid spheroids of disparate size, followed by fragmentation. In some instances, complex porous microstructures with *matreshka* ("Russian doll") morphologies were observed (Figure 9). These could originate from the aggregation and fusion of two large polyperforated microspheres followed by surface infilling at the contact point, or through the distortion of a large single sphere and disengagement at the contact point.

Polyindented silica/gold microspheres were also prepared from sonicated water/toluene dispersions (35 μL/100 mL) containing 2:1 nanoparticle mixtures, respectively, at increased temperatures of 10−20 °C. The spheroids were polydisperse in size with a peak in the population density around 0.75 μm that extended at low-

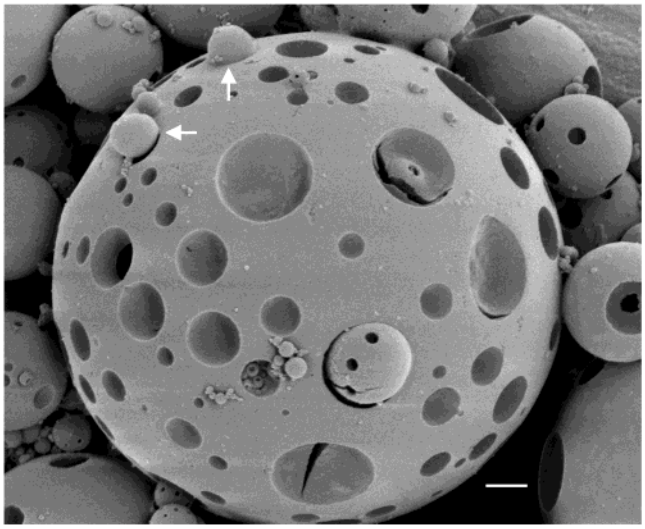

Figure 8. SEM images showing 12-μm-diameter silica/gold microsphere with polyindented morphology prepared at 0 °C with reduced water content (17.5 μL). Arrows show presence of residual surface-fused smaller microspheres that are responsible for the impact craters. Scale bar = 1 μm.

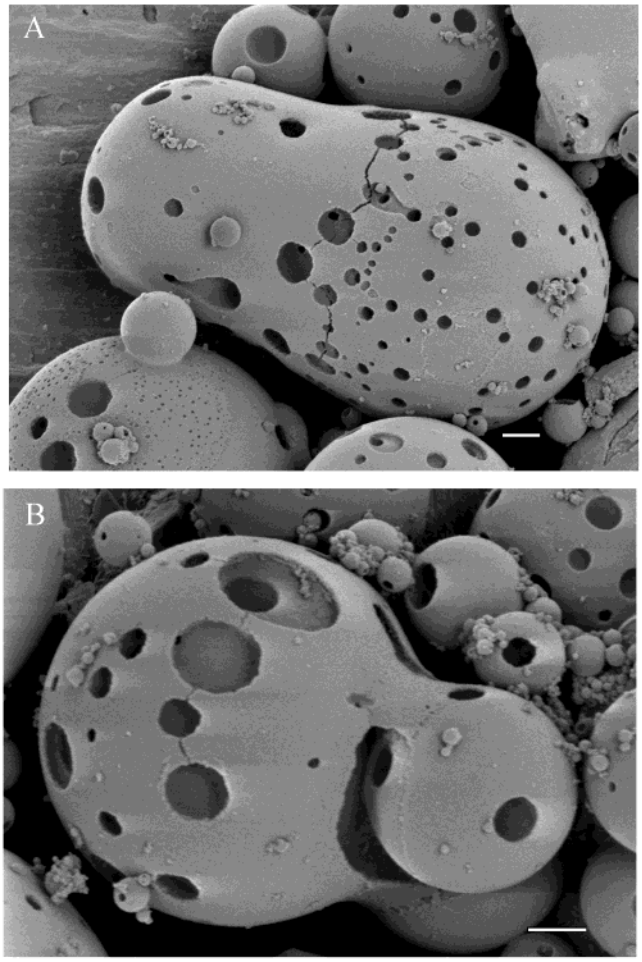

Figure 9. SEM images of "Russian doll" silica/gold microstructures prepared at 0 °C with reduced water content (17.5 μL): (a) intact form, and (b) broken structure showing interior consisting of a fused pair of polyindented microspheres. Scale bars = 1 μm.

frequency values up to diameters of 20 μm. The large microspheres showed a variety of remarkable surface textures, such as a golf ball-like morphology consisting

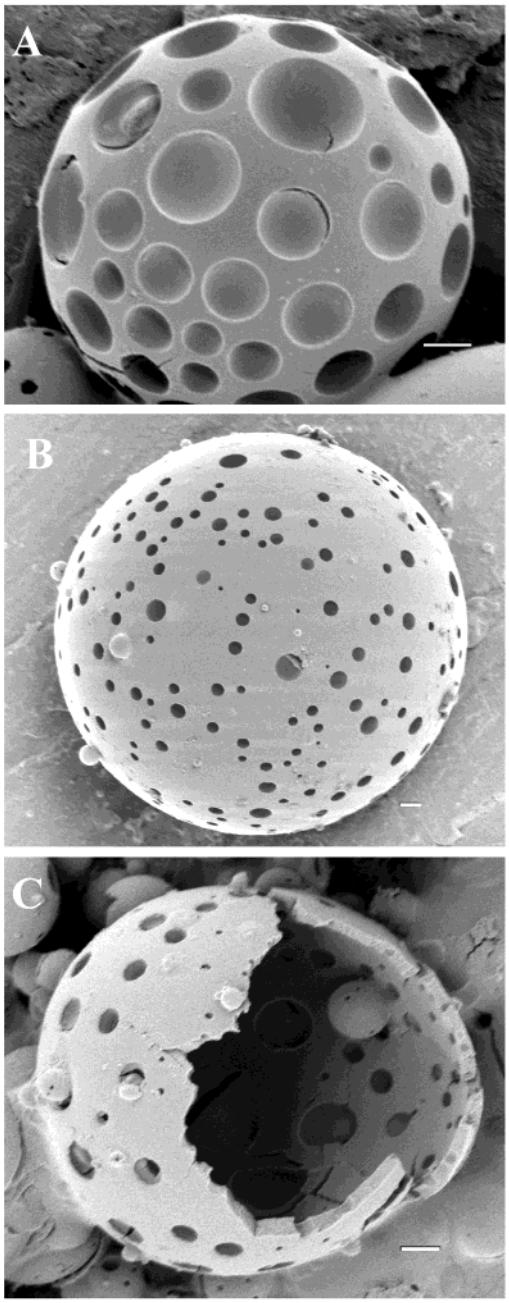

Figure 10. SEM images showing silica/gold microspheres with polyindented morphology prepared at 10 °C with 35 μL of water: (a) golf-ball-like form; (b) sphere with surface perforations; and (c) fractured microsphere showing hollow interior. Scale bars = 1 μm.

of closely packed micron-sized circular indentations (Figure 10a). Other spheroids showed surface indentations that were perforated (Figure 10b), indicating that structures were often hollow and surrounded by a thin wall of densely packed gold and silica nanoparticles. Corresponding SEM images of fractured samples indicated that the hollow microspheres often consisted of a large single internal cavity (Figure 10c), although interiors with foamlike structure were also observed. Decreasing the amount of gold in the nanoparticle mixture (SiO_2:Au = 10:1) did not significantly change the morphology or size distribution of the microspheres but reduced the size of the surface indentations and holes. All the above morphologies remained unchanged when microspheres were placed in polar solvents or heated to 450 °C.

The above results indicate that the formation of the pitted olive morphology is favored for microspheres/water droplets of similar size, whereas mixtures of large and small microspheres with multiple and single indentations, respectively, are produced when solidification of the nanoparticle-containing droplets occurs prior to homogenization of the emulsion (Figure 11). The rate of solidification can be increased by various experimental conditions. For example, water contents less than 20 μL are expected to be below the saturation value for dissolution in toluene at 0 °C, with the consequence that the droplet volume is decreased rapidly and solidification occurs before uniform-sized droplets are formed by prolonged sonication. Polydisperse microspheres are also observed at 0 °C when the sonication time is reduced to 2.5 min at a water content of 35 μL/100 mL toluene (data not shown), indicating that at least 3 min is required to establish a homogeneous dispersion of micrometer-sized water droplets under these conditions. Raising the temperature to 10 °C also increases the rate of solidification due to the increased solubility of water in toluene, with the consequence that polyindentated microspheres are produced according to the above mechanism.

General Discussion and Conclusions

The results described in this paper indicate that gold, silica, or silica/gold nanoparticle-containing microspheres can be readily assembled within dissolving water droplets dispersed in toluene. For a given solids content, the water concentration, temperature, and sonication time determine the rate and extent of dissolution, which influence the rate of solidification and internal structure of the microspheres. A very low water content (and relatively high temperature) results in complete dissolution and solidification prior to the formation of similar-sized droplets in the emulsions. This increases the microsphere polydispersity and tends to produce dense solid structures. Intermediate levels of water and low temperatures slow the rate of nanoparticle consolidation and favor microspheres with similar size and solid or hollow interiors, provided that the sonication time is sufficiently long. In contrast, high levels of water well above the saturation limit give nonrigid hollow inorganic structures due to high residual water contents. This prevents solidification in the water droplets even after extended sonication times, with the consequence that the structures collapse during sample preparation (data not shown).

A key result of the current work is that the nanoparticle composition of the water droplets significantly influences the degree to which interparticle collisions and aggregation are transcribed into the microsphere morphology during the solidification process. Spheroids prepared from gold or silica nanoparticles alone are smooth and show no or little evidence of interparticle fusion/fragmentation. In contrast, the presence of 30−70 wt % Au within the silica matrix significantly modifies the chemical and mechanical properties of the

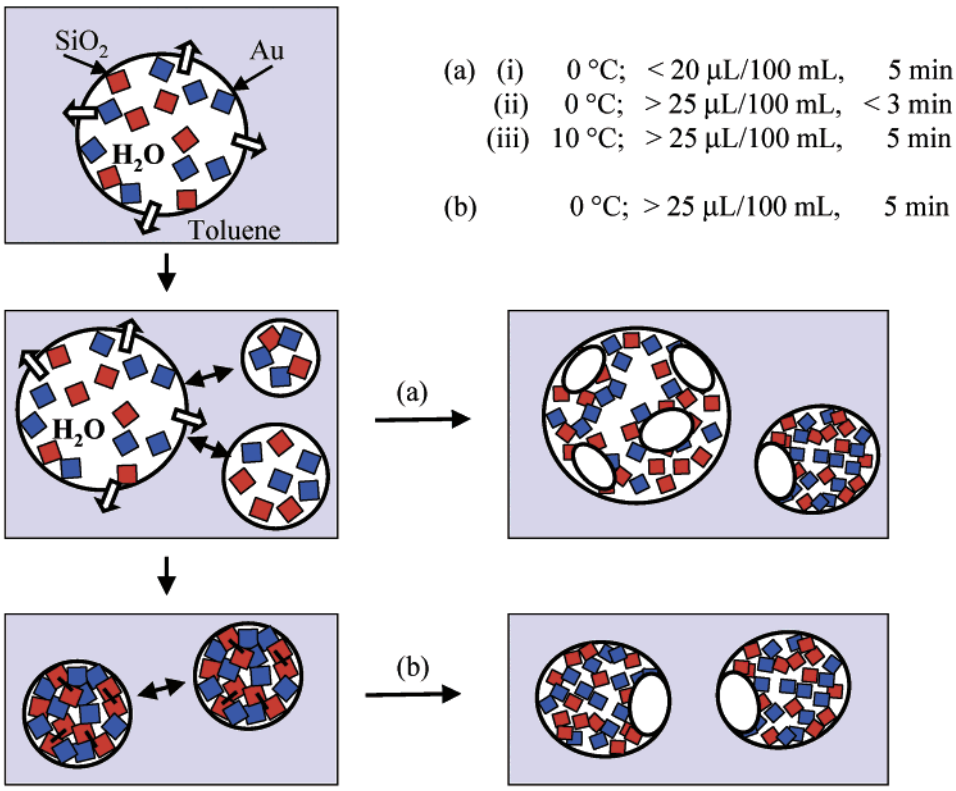

Figure 11. Scheme showing relationship between dispersity of water droplets in toluene and formation of nanoparticle-containing microspheres with complex forms. Left side of the drawing shows initial formation of polydisperse nanoparticle-containing droplets that become more homogeneous (bottom left) with prolonged sonication. Rapid solidification or insufficient sonication time (condition (a)) results in replication of the highly polydisperse state and formation of multiply indented large microspheres and smaller spheroids with single holes (middle right). In contrast, slower rates of solidification (condition (b)) give rise to particles with similar diameters that undergo binary collisions to produce microspheres with pitted olive morphology (bottom right).

microspheres such that interactions between particles result in surface patterning. We propose that in the case of pure gold, the microspheres behave as noninteracting spheres because the constituent nanoparticles are held together by capillary forces and are chemically inert with respect to interparticle cross-linking. In contrast, silica nanoparticles are rapidly gelled to produce microspheres that are surface-active, with the consequence that interactive collisions can occur between the spheroids. For pure silica, however, collisions between the microspheres are not imprinted in the surface texture. This suggests that the surfaces are sufficiently soft, flexible, and/or fluid during collisions to accommodate reversible binding and release without disruption of the surface morphology.

Addition of gold nanoparticles into the silica matrix appears to significantly change the surface and bulk properties of the inorganic deposits such that collisions between the incipient microspheres result in conjoined spheroids, which subsequently fragment leaving circular surface indentations and holes. One possibility is that the hardness and surface fluidity of the composite microspheres are modified to levels intermediate between the pure gold and silica phases, such that interparticle adhesion is associated with significant mechanical disruption of the interface. For the pitted olive morphology, the single indentation observed after fragmentation suggests that the fused pairs are initially in the form of water-filled inorganic shells with similar wall thickness. Loss of solvent and further consolidation of the nanoparticles occurs around the surface of the conjoined hemispheres except at the interfacial region where the droplets become continuous. Thus, an internal cavity is produced specifically across the interface as the nanoparticles are compacted against the shrinking surfaces of the coupled droplets. Subsequent breakage at the point of contact then reveals the cavity as a single indentation in each hemisphere.

In contrast, the large polyindented microspheres exhibit a variety of surface features, suggesting that the multiple collisions involve spheroids of varying size and shell thickness. As the water solubility increases with decreasing droplet size, the smaller spheroids solidify first and therefore are likely to be harder than the thin inorganic walls that surround larger droplets of the nanoparticle dispersion. As a consequence, the larger microspheres are subjected to extensive bombardment by small dense spheroids that produce micron-sized "impact craters" across the surface during solidification.

In conclusion, we have demonstrated that sonication of microliter volumes of aqueous silica, gold, or silica/gold colloids in toluene results in the facile preparation of nanoparticle-based microspheres. Mixtures of silica and gold at a weight ratio of 2:1 have a pronounced effect on the surface and bulk properties of the assembled microstructures such that nanocomposite microspheres with complex morphologies (pitted olives/polyindented spheroids) are produced by higher-order aggregation. The complex forms are associated with changes in the collision dynamics that are influenced by the rate of solidification, which increases for higher

levels of water solubility. Although further work is required to explain mechanistically how such dramatic modifications in aggregation/fusion can arise from compositional changes, the methodology should be applicable to a wide range of inorganic nanoparticles for use in catalysis, separation science, and bioengineering. Studies on the sonication-induced water-droplet assembly of magnetite and titania nanoparticles into microspheroidal materials are currently being undertaken.

Acknowledgment. We thank the EPSRC, UK, for financial support, the European Union for a Marie Curie Individual Fellowship (HPMF-CT-1999-00254) to E.D., and Dr. C. Boissiere for scientific discussions.

CM021259E